SATBAYEV UNIVERSITY

Journal of Energy, Mechanical Engineering and Transport

Volume 1 (2024), Issue 3, 20-25

https://doi.org/10.51301/jemet.2024.i3.04

Simulation of heat treatment and combustion of fuel in an external vortex burner

R. Shylmagambetov*, B. Ongar

Satbayev University, Almaty, Kazakhstan

**Corresponding author: raha210500@gmail.com*

Abstract. This comprehensive article delves into the intricate processes associated with the heat treatment and combustion of fuel in an external vortex burner. Encompassing a diverse array of facets within the topic, the research extends to include a meticulous analysis of heat flow, exploration of combustion characteristics, and the pursuit of optimal process configurations. Leveraging the power of numerical models, this research enables a more profound comprehension and articulation of the intricate interplay between fuel, air, and combustible substances within the burner. The outcomes of this study hold tangible implications for the practical advancement of combustion systems, promising enhanced efficiency, reduced emissions, and streamlined processes in the expansive realm of the energy industry. The article thoughtfully incorporates references to contemporary scientific research, presenting the findings derived from numerical simulations. These findings not only contribute substantively to the existing body of knowledge but also lay the groundwork for prospective research endeavors and practical implementations in the dynamic domain of heat treatment and fuel combustion within external vortex burners.

Keywords: *heat treatment modeling, vortex burner, heat transfer in the burner, heat flows, thermodynamics, fuel combustion efficiency.*

1. Introduction

Modeling the thermal treatment and combustion of fuel in an external vortex burner is a crucial and dynamic area of ongoing research. This focus on investigation is fueled by the tremendous potential it holds for fostering a profound comprehension of the intricate physical processes unfolding within the burner. Moreover, it serves as a gateway for optimizing the burner's operation, factoring in a myriad of influential variables.

The primary objective of this comprehensive study is to meticulously craft and employ advanced numerical models. These models are tailored for a multifaceted analysis, encompassing the examination of heat flows, combustion characteristics, and the overall optimization of the fuel combustion process within an external vortex burner. The intricacies of heat flow modeling empower researchers to assess the nuanced distribution of heat within the burner, thereby discerning the efficacy of heat transfer.

Equally vital is the examination of combustion characteristics, offering a profound exploration into fuel combustion processes. This includes scrutinizing critical parameters such as combustion rate, combustion efficiency, and the generation of emissions. The overarching aim of optimizing the fuel combustion process in an external vortex burner is laser-focused on augmenting combustion efficiency, curtailing emissions, and establishing a more steadfast operational framework for the entire system.

Within the confines of this article, an exhaustive overview of existing research in the realm of modeling thermal treatment and combustion of fuel in an external vortex burner will be presented. Additionally, the findings arising from our bespoke numerical simulations will be disclosed, accompanied by a thorough discussion of their tangible implications for the energy industry. It is anticipated that the outcomes and deductions put forth in this article will serve as valuable assets for the advancement of more resourceful fuel combustion systems. This encompasses not only the reduction of harmful emissions but also the fine-tuning of heat treatment processes within an external vortex burner.

Recognizing the broader significance of attaining a comprehensive understanding of fuel combustion processes and their intricate modeling within an external vortex burner, it becomes evident that these endeavors hold paramount importance. Such endeavors are pivotal in steering our collective trajectory towards the realization of a sustainable and environmentally friendly energy system, aligning with the imperatives of our time.

2. Materials and methods

2.1. Tools and materials

The experimental combustion chamber comprises four principal components, delineated as the exhaust fan, gas pipe, swirler, and combustion chamber, as illustrated in Figure 1. The primary airflow is facilitated by the exhaust fan, while the gas pipe, connected to the gas pipeline, serves as the conduit for transporting the fuel, specifically natural gas. The furnace is characterized by a vaulted chamber configuration, featuring a transition cylinder at the inlet. The overall length of the furnace is 11.290 mm.

To facilitate temperature measurements within the furnace, thermocouples are strategically installed at each control point. These thermocouples, denoted as T in Figure 1, pro-

vide crucial data on the temperature distribution within the experimental setup. Notably, a Cartesian coordinate system is established, with its origin situated at the center of the combustion chamber outlet. This coordinate system aids in spatial referencing and analysis, contributing to a systematic understanding of temperature variations and combustion characteristics throughout the combustion chamber. The integration of thermocouples at key locations enhances the precision of temperature measurements, enabling a comprehensive assessment of the thermal performance within the experimental combustion chamber.

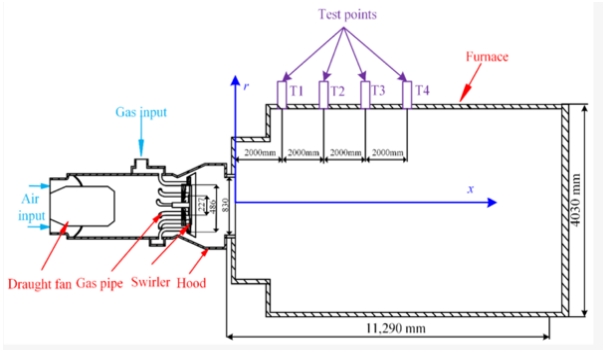

Figure 1. Scheme of combustion chamber geometry

As depicted in Figure 2a, the swirler employed in this study adopts a double concentric configuration, comprising a first stage blade and a second stage blade. Gas nozzles are strategically positioned at regular intervals around the circumference of the second stage blade. This intricate design promotes a dynamic airflow pattern within the swirler, where the air passing through it is divided into two distinct jets: a rotating jet generated by the swirling motion and a straight jet formed by the remaining air. The synergistic action of these jets contributes to the overall combustion dynamics within the system.

Figure 2b further illustrates the specific swirler utilized in the experiment-a unidirectional rotating swirler. This design choice introduces additional precision and control into the experimental setup, enabling a more targeted investigation of combustion processes.

For a comprehensive understanding of the experimental framework, Table 1 provides specific design parameters of the combustion chamber. These parameters serve as crucial benchmarks, offering insights into the foundational elements that influence the combustion characteristics under scrutiny. This detailed overview sets the stage for a nuanced exploration of the interactions between swirler design, airflow dynamics, and combustion behavior within the defined experimental context.

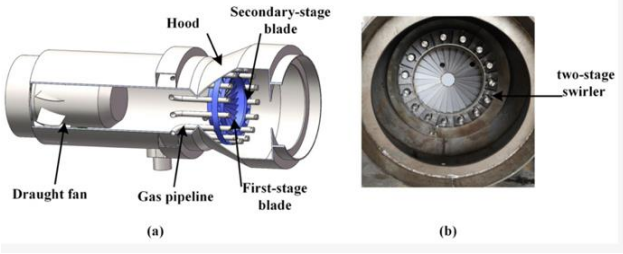

Figure 2. a) Schematic diagram of the three-dimensional design of a two-stage swirler; (b) two-stage swirler used in the present experiments

Table 1. Combustion chamber parameters

Parametres	Values
Combustion chamber outlet diameter (mm)	830
Number of blades in the first stage	28
Number of blades in the second stage	30
First stage blade angle (°)	60
Second stage blade angle (°)	65
Blade thickness (mm)	1

2.2. Research methodology

The swirler is usually characterized by the twist number S, and the twist number S is used to reflect the rotational force [1]. This dimensionless quantity is defined as the ratio between the axial flux of angular momentum Gφ and the axial flux of axial momentum Gx and is defined as [1]:

$$S = \frac{G_\varphi}{G_x R} \tag{1}$$

where R usually represents the radius of the jet exit.

The chord length l and the blade angle β for the axial swirler are constant, so the axial velocity over the cross section can be distributed approximately evenly. Taking $R = R_1$, a simplified expression for calculating the number of vortices has the form [1]:

$$S = \frac{2}{3}\left(\frac{1-(\frac{R_0}{R_1})^3}{1-(\frac{R_0}{R_1})^2}\right)\tan\beta \tag{2}$$

where β is the blade angle between the normal direction of the blade and the airflow direction, and R_0 and R_1 are the inner and outer radii of the blade, respectively.

The entire experimental setup is designed for both cold flow and combustion experiments. According to the experimental specification requirements, the frequency of the exhaust fan is adjusted by the data measured by the pitot tube (product model number: JY-GD680) to achieve the same air intake boundary conditions. Vortex flow meter (HP-LUX-DN100YF3E1B1) monitors methane flow, the accuracy is 1% of the measurement range. The temperature distribution inside the combustion chamber is measured by a 300mm long thermocouple (platinum-rhodium alloy thermocouple, S type product model number: WRP-130). Measuring range 0–1600°C, measurement accuracy ±6°C. Emission concentrations were obtained with a gas analyzer probe (Testo-350). The sampling probe was installed at the outlet of the combustion chamber. Measuring range 0-500 ppm, resolution 0.1 ppm, accuracy ± 2 ppm. Other parameters used throughout the experiment are given in Table 2. The burner fuel is natural gas, and its main component is methane. For an ideal incompressible gas, the inlet velocity is taken at the inlet and the outlet pressure is taken at the outlet. The non-slip boundary is adopted on the surface of the burner wall and the surface of the furnace wall [2].

Table 3 presents a detailed comparison between the experimentally measured temperatures and the results derived from numerical simulations. Remarkably, the numerical error between these two sets of data remains under 10%, affirming the robustness and reliability of the simulation outcomes. This validation underscores the credibility of the values se-

lected in this paper, reinforcing their appropriateness for subsequent analysis and interpretation.

In Figure 3, the visual representation of the burner flame's configuration within the furnace during the experiment is showcased. This depiction offers a tangible insight into the dynamic nature of the combustion process under study. The visual evidence further complements the quantitative temperature comparisons, providing a holistic understanding of the burner's performance in the experimental setting. These combined analyses contribute to a comprehensive evaluation of the simulation results, enhancing the overall confidence in the reliability and accuracy of the chosen parameters and values for the purpose of this study.

Table 2. Combustion chamber parameters

Parameters	Values
Inlet air speed (m/s)	18.92
Air intake diameter (m)	0.35
Inlet gas velocity (m/s)	28
Gas inlet diameter (m)	0.141
Atmospheric temperature (K)	298
Inlet air temperature (K)	298
Excess air coefficient	1.18
Outlet pressure (Pa)	-70

Figure 3. Burner flame in the furnace during the experiment

Table 3. Comparison of experimental and numerical simulation results

Thermocouple number	Experiment (°)	Calculation (°)	Error
T1	798	827	3.6 %
T2	1092	998	8.6 %
T3	985	956	2.9 %
T4	967	1008	4.2 %

3. Results and discussion

In Figure 4a, the schematic presents the design of a two-stage cyclone characterized by blade angles of 65° for the first stage and 20° for the second stage. This section of the article draws on the conceptualization of the D65-30 engine, incorporating gas classification combustion technology to inform crucial design decisions. An evolved cyclone design, denoted as CD65-30, is introduced in Figure 4, featuring additional structures such as a central gas pipeline and gas injectors. Notably, this enhanced design incorporates a total of 12 injectors—six central gas injectors and six peripheral gas injectors.

The rationale behind this improved design is twofold. Firstly, it aims to boost the efficiency of heat transfer between the flame and the unit by optimizing the combustion of gas and air at the upper section of the furnace. Secondly, it facilitates fuel distribution, wherein adjustments to the gas-to-air equivalent ratio in the primary air zone are made. The combustion in the primary blade zone is meticulously fine-tuned using the gas classification combustion method. The efficacy of these design enhancements is substantiated by computational fluid dynamics (CFD) simulations of burner flow, providing detailed insights into axial and radial velocity distributions at various burner positions.

This comprehensive approach aligns with the overarching goal of refining combustion dynamics, ensuring effective heat transfer, and optimizing fuel-air mixtures for efficient combustion. The integration of advanced design elements, supported by CFD simulations, underlines a commitment to precision and innovation in the pursuit of enhanced burner performance within the specified experimental framework.

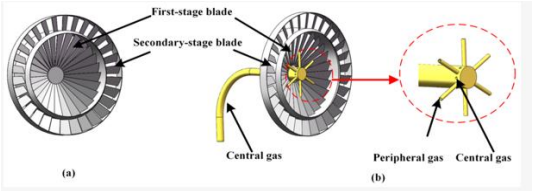

Figure 4. Three-dimensional structure of (a) D65-30 and (b) CD65-30

Examining Figure 5a reveals a distinctive feature near the termination of the central gas pipe for CD65-30—a recirculation zone formed by the high-speed airflow through the gap between the swirler and the central gas pipe. The spatial extent of this region is remarkably small, as illustrated in Figure 5b. Moving on to Figures 5c and 5d, a comparative analysis demonstrates that the recirculation zone generated at the periphery of CD65-30 surpasses that of D65-30 in both size and prominence. This augmentation in the recirculation zone for CD65-30 contributes to an enhanced flame stability.

Furthermore, it is noteworthy that the axial speed of D65-30 surpasses that of CD65-30. This discrepancy in axial speed, with D65-30 exhibiting higher values, introduces a nuanced dynamic. The higher axial speed in D65-30 is deemed unfavorable for the objective of shortening the flame front length. This observation underscores the intricate relationship between burner configurations, airflow patterns, and their consequential impact on flame characteristics. The expanded recirculation zone in CD65-30, coupled with a more favorable axial speed, collectively signifies improved flame stability, presenting valuable insights into the interplay of design parameters in optimizing burner performance.

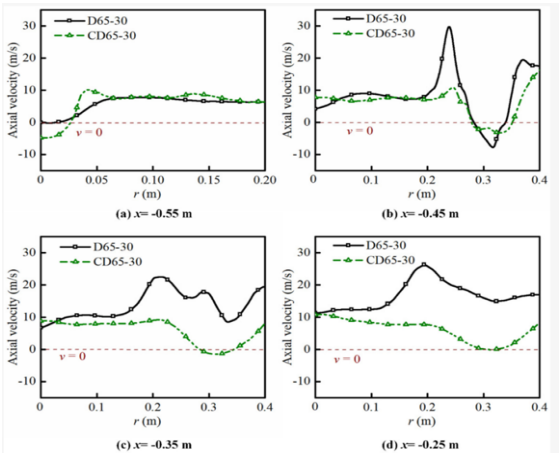

Figure 5. Axial speed of D65-30 and CD65-30 at different axial positions

From Figure 6a, it can be seen that the tangential velocity of CD65-30 increases, then decreases, and then increases again in the radial direction in this region (x = -0.55 m). The peak tangential velocity occurs in the area where the radial distance is less than 0.05 m. This is the reflux zone near the central gas pipe. The influence of the central recirculation zone makes the overall tangential velocity of CD65-30 less than that of D65-30. From Figures 6b–d it can be seen that the secondary wind region creates a negative tangential speed, that is, the direction of rotation of the air flow here is opposite to the direction of rotation of the main air flow. The reason is that the angles of the primary blade and the secondary blade are different after the cyclone blade, and there is a tangential speed difference.

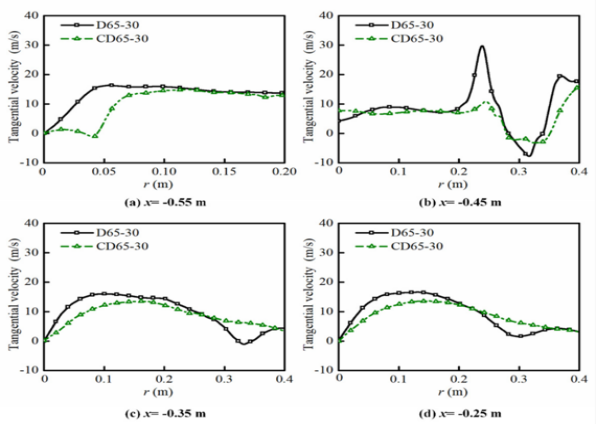

Figure 6. Tangential velocity of D65-30 and CD65-30 at different axial positions

In Figure 7 it can be seen that the nozzles are located in such a way that gas and air are additionally mixed for CD65-30, and intense mass-energy exchange occurs in the boundary layer between the two regions. The energy generated by combustion in the central part of the pipe is gradually transferred to the periphery, which contributes to the stability of the flame. Compared to the flame length, it is found that the difference between them is very small. Unlike the D65-30, the gas injected by the central nozzle burns at the bottom of the cyclone and forms a narrow high-temperature zone. The location of the CD65-30 gas injectors in the burner casing allows for further uniform mixing of gas and air with intense exchange of mass and energy at the boundary layer between two zones of highly turbulent combustion. For CD65-30, a high-temperature flue gas generated by combustion in the central zone, the energy contained in the flue gas is transferred to the periphery in stages, which is beneficial for stabilizing the flame. The heat generated by D65-30 after combustion in the peripheral zone of the secondary air is more transferred to the peripheral environment due to strong turbulence, and only a small amount of thermal energy diffuses inward.

Comparing the temperature at the furnace wall from Figure 8, the temperature of D65-30 is slightly higher than that of D65-30, which means that installing a nozzle does not significantly improve the efficiency of heat exchange between the flame and the firebox. unit. The position against the wall is also where the thermocouple is installed on the top wall of the combustion chamber.

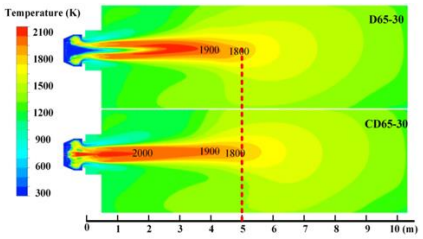

Figure 7. Tangential velocity of D65-30 and CD65-30 at different axial positions

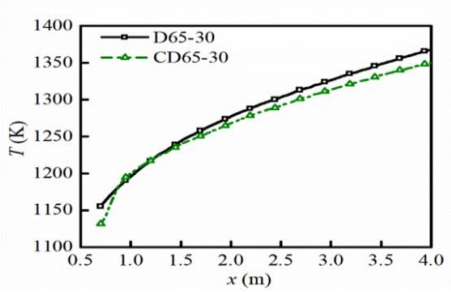

Figure 8. Temperature distribution of D65-30 and TsD65-30 near the furnace wall

Examining Figure 9 provides a clear distinction between the NOx concentrations of D65-30 and CD60-30 within the oven chamber. Notably, D65-30 exhibits an overall higher NOx concentration, marked by a substantial zone behind the burner where NOx concentrations exceed 70 ppm. To contextualize this finding, a comparison with temperature profiles in Figure 7 unveils that this region of elevated NOx concentration aligns downstream of the high-temperature zone in the furnace chamber, where local temperatures surpass 2000 K. The rapid conversion of nitrogen in the air to thermodynamic NOx in response to these heightened temperatures explains the prevalence of high NOx concentrations in this specific zone for D65-30.

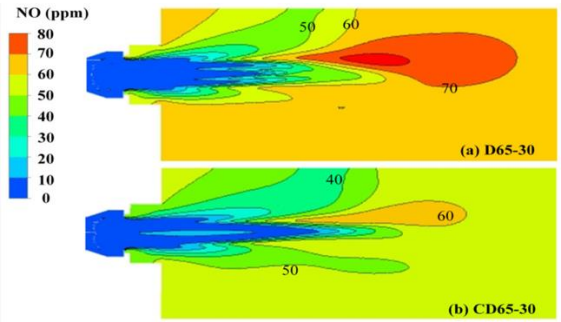

Figure 9. Local distribution of NOx concentration (ppm) D65-30 and CD65-30 on the central cross section

Conversely, CD65-30 also manifests an area with elevated local NOx concentration in the same region. However, it is noteworthy that both the spatial extent and magnitude of this area are comparatively smaller when juxtaposed with the corresponding region in D65-30. This nuanced observation suggests that the CD65-30 configuration exhibits a more controlled and mitigated distribution of NOx concentrations in the high-temperature zone, highlighting its potential to curtail the formation of nitrogen oxides in comparison to the D65-30 counterpart.

In essence, the detailed analysis of NOx concentrations in relation to temperature profiles underscores the intricate interplay between burner design and resultant combustion dynamics. These findings not only shed light on the specific areas of concern but also underscore the effectiveness of CD65-30 in managing and mitigating NOx emissions, thereby contributing to a more nuanced understanding of the impact of burner configurations on combustion performance.

Examining Table 4 reveals a noteworthy distinction in the NOx concentration between the CD65-30 and the D65-30 at the furnace outlet. This discrepancy is attributed to the implementation of staged combustion of gas, facilitated by the introduction of a central gas nozzle and a sophisticated multi-stage layered arrangement of nozzles. These design enhancements not only contribute to the combustion efficiency but also enable additional dilution of the fuel, resulting in a discernible reduction in the NOx concentration at the furnace outlet for the CD65-30 compared to the D65-30 configuration. This insightful observation underscores the efficacy of strategic design modifications in curbing NOx emissions, emphasizing the potential of advanced burner configurations in achieving more environmentally sustainable combustion processes.

Table 4. Comparison of experimental and numerical simulation results

Name	NOx concentration
D65-30	70.8
CD65-30	57.3

4. Conclusions

Expanding on the investigation into the NOx strategy for staged burners and the optimal design of natural gas burners, our research integrates a comprehensive approach, leveraging both computational fluid dynamics analysis and experimental validation. The key findings from this study are outlined as follows:

Implementation of a central gas nozzle, employing a two-stage vortex design, yields a notable reduction in NOx concentration, decreasing from 70.8 to 57.3. This reduction is achieved while maintaining nearly constant air flow across all stages, courtesy of gas-stage combustion technology. It is noteworthy, however, that the flame front length, flame stability, and heat transfer efficiency exhibit marginal changes.

A thorough parametric analysis of a two-stage swirler blade reveals that adjusting the inclination angle of the second-stage blades, while keeping the first-stage blades' angle constant, has significant effects. A decrease in the second-stage blade inclination angle diminishes the tangential velocity of the overall air flow, thereby weakening the mixing effect of gases within the two-stage swirler. As the second-stage blade angle decreases, the flame front length undergoes a gradual reduction, accompanied by a decline in flame stability and a subsequent increase in NOx concentration. Interestingly, reducing the inclination angle of the second-stage blade initially leads to a decrease in heat transfer efficiency, followed by a subsequent increase.

In pursuit of flame stabilization and a reduction in flame front length, a novel blunt body design, denoted as D65-C45, is introduced. This design effectively lowers the NOx concentration at the furnace outlet to 64.9, corresponding to a reduced flame front length of approximately 4.8 meters. This innovative approach demonstrates its efficacy in achieving both flame stability and NOx reduction.

In summary, our investigation underscores the multifaceted nature of optimizing natural gas burners, emphasizing the interplay between design parameters, combustion dynamics, and emission control. The proposed modifications, including the two-stage vortex design and the novel blunt body design, showcase promising results in achieving enhanced combustion performance and reduced environmental impact.

References

[1] Huang, L., Kumar, K. & Mujumdar, A. S. (2004). Simulation of a spray dryer with a rotating disk atomizer using a 3D computational fluid dynamics model. *Sukhoi, 22*, 1489–1515

[2] Edland, R., Normann, F., Fredriksson, K. & Andersson, K. (2017). Implications of fuel selection and burner settings on combustion efficiency and NOx formation in PF iron ore rotary kilns. *Energy Fuel, 31, 3253–3261*

[3] Fan, X., Liu, K., Xu, G., Zhang, K., Wang, J. & Lin, Y. (2020). Experimental studies on the atomization structure and interaction between sectors of a low-emission dual-vortex combustor. *Chin. J. Aeronaut., 33, 204–212*

[4] National Agency for Renewable Energy of Kazakhstan. (2017). Analysis of the efficiency of using wind for the production of electricity

Сыртқы бұрандалы оттықттың термиялық өңдеу мен отын жағуды моделдеу

Р. Шылмагамбетов*, Б. Онгар

Satbayev University, Алматы, Қазақстан

**Корреспонденция үшін автор: raha210500@gmail.com*

Аңдатпа. Бұл мақалада сыртқы бұрандалы оттықтағы отынның термиялық өңдеуі және жануымен байланысты күрделі процестер қарастырылады. Тақырыптың әр түрлі қырларын қамтитын зерттеу жылу ағынының мұқият талдауын, жану сипаттамаларын зерттеуді және оңтайлы процесс конфигурацияларын іздеуді қамтиды. Сандық үлгілердің күшін пайдалана отырып, бұл зерттеу оттық ішіндегі отын, ауа және жанғыш заттар арасындағы күрделі өзара әрекетті тереңірек түсінуге және артикуляциялауға мүмкіндік береді. Бұл зерттеудің нәтижелері жану жүйелерінің практикалық ілгерілеуіне айтарлықтай әсер етеді, энергетикалық саланың кең ауқымында тиімділікті арттыруды, шығарындыларды азайтуды және процестерді оңтайландыруды болжайды. Мақалада қазіргі заманғы

ғылыми зерттеулерге сілтемелер мұқият енгізілген, сандық модельдеуден алынған нәтижелер ұсынылған. Бұл тұжырымдар бар білімдер жиынтығына айтарлықтай үлес қосып қана қоймайды, сонымен қатар сыртқы құйынды оттықтардағы термиялық өңдеу мен отынды жағудың динамикалық саласындағы перспективалық зерттеулер мен практикалық енгізулер үшін негіз қалады.

Негізгі сөздер: *термоөңдеу модельдеу, бұрандалы оттық, оттық жылу беру, жылу ағындары, термодинамика, отынның жану тиімділігі.*

Моделирование термической обработки и сжигания топлива во внешней вихревой горелке

Р. Шылмагамбетов*, Б. Онгар

Satbayev University, Алматы, Казахстан

**Автор для корреспонденции: raha210500@gmail.com*

Аннотация. Данная статья посвящена моделированию процессов термической обработки и сжигания топлива во внешней вихревой горелке. Исследование охватывает различные аспекты данной темы, включая анализ тепловых потоков, характеристики сгорания и оптимизацию процесса. Применение численных моделей позволяет более глубоко понять и описать взаимодействие топлива, воздуха и горючего вещества в горелке. Результаты исследования имеют практическую значимость для разработки более эффективных систем сжигания топлива, снижения выбросов и оптимизации процессов энергетической отрасли. В статье представлены ссылки на актуальные научные исследования и приводятся результаты численных моделирований, которые могут служить основой для дальнейших исследований и практических применений в области термической обработки и сжигания топлива во внешней вихревой горелке.

Ключевые слова: *моделирование термической обработки, вихревая горелка, теплопередача в горелке, тепловые потоки, термодинамика, эффективность сжигания топлива.*

Received: 15 May 2024
Accepted: 15 September 2024
Available online: 30 September 2024